November, 2018

Reactive Ion Plasma Modification of Poly(Vinyl-Alcohol) Increases Primary Endothelial Cell Affinity and Reduces Thrombogenicity

Patrick L. Jurney, *San Jose State University*
Deirdre E.J. Anderson, *Oregon Health & Science University*
Grace Pohan, *University of Waterloo*
Evelyn K.F. Yim, *University of Waterloo*
Monica T. Hinds, *Oregon Health & Science University*

Reactive ion plasma modification of poly(vinyl-alcohol) increases primary endothelial cell affinity and reduces thrombogenicity

Patrick L. Jurney
Department of Biomedical Engineering,
Oregon Health & Science University
Portland, Oregon 97239
jurney@ohsu.edu

Deirdre E. Anderson
Department of Biomedical Engineering,
Oregon Health & Science University
Portland, Oregon 97239
anderdei@ohsu.edu

Grace Pohan
Department of Chemical Engineering,
University of Waterloo
Waterloo, Ontario, Canada
gpohan@uwaterloo.ca

Evelyn K.F. Yim
Department of Chemical Engineering,
University of Waterloo
Waterloo, Ontario, Canada
eyim@uwaterloo.ca

Monica T. Hinds
Department of Biomedical Engineering,
Oregon Health & Science University
Portland, Oregon 97239
hindsm@ohsu.edu

Abstract

Bulk material properties and luminal surface interaction with blood determine the clinical viability of vascular grafts and reducing intimal hyperplasia is necessary to improve their long-term patency. Here we report that the surface of a biocompatible hydrogel material, poly(vinyl alcohol) (PVA) can be altered by exposing it to reactive ion plasma (RIP) in order to increase primary endothelial cell attachment. We varied the power and the carrier gas of the RIP treatment and characterized the resultant surface nitrogen, water contact angle, as well as the ability of the RIP treated surfaces to support primary endothelial colony forming cells. Additionally, in a clinically relevant shunt model, the amounts of platelet and fibrinogen attachment to the surface were quantified during exposure to non-anticoagulated blood. Treatments with all carrier gases resulted in an increase in the surface nitrogen. Treating PVA with O_2, N_2, and Ar RIP increased affinity to primary endothelial colony forming cells. The RIP treatments did not increase the thrombogenicity compared to untreated PVA and had significantly less platelet and fibrinogen attachment compared to the current clinical standard of ePTFE. These findings indicate that RIP-treatment of PVA could lead to increased patency in synthetic vascular grafts.

1. Introduction

Cardiovascular disease is the leading cause of death globally[1]. In the United States alone approximately 400,000 coronary artery bypass grafting procedures are performed annually.[2] Autologous vasculature is the preferred bypass graft material for treating both coronary heart disease as well as critical limb ischemia due to its superior clinical performance, as measured by long-term patency. However, half of all autologous vessels fail by year 10, and many patients in need of bypass grafts lack suitable autologous vessels to chronic disease and/or previous interventions.[3,4] Hence, there is a critical need for an alternative to autologous bypass graft materials. Graft material properties affect long-term patency *in vivo* and therefore should be taken into account when considering a synthetic graft biomaterial. One factor responsible for the failure of the majority of small diameter vascular implants is the interaction between the luminal surface of the graft and blood which lead to thrombosis and intimal hyperplasia.[5]

Cell-derived extracellular matrix (ECM) and synthetic materials have been studied as vascular graft biomaterials.[6,7] Several ECM materials have shown promise in improving biointegration after decellularization, but the techniques used to decellularize ECM including osmotic shock, detergents, proteolytic digestions, and DNase/RNase treatment have drawbacks associated with loss of important components of the native structure of ECM.[8] Decellularized ECM biomaterials may also be taken from a biological specimen, most commonly whole vessels[9] or porcine submucosa,[10] and therefore have limits on manufacturing reliability, in addition to being subject to variables such as the age and pathological conditions of the donor.[8] Synthetic graft biomaterials have been studied as alternatives to autologous grafts with considerable success in large- (>8 mm) and medium-diameter arteries (6-8 mm).[11,12] However small-diameter (<6 mm) synthetic grafts have historically suffered from clinically unacceptable failure rates which restrict their adoption in the clinic.[7] In the case of the current clinical standard, expanded polytetrafluoroethylene (ePTFE), half of all small diameter synthetic bypass grafts fail within two years of implantation,[7] and thus, are not typically used in coronary artery bypass surgery, for example.[13] Polymeric materials such as ePTFE offer the benefits associated with reproducible manufacturing processes but are most often designed to be biologically inert, specifically exhibiting material hydrophilicity with a negative surface charge, in order to avoid thrombogenesis and neointimal hyperplasia.[14] Studies have shown that inert synthetic materials can be sufficiently non-thrombogenic,[15] particularly in the presence of recommended anti-coagulant drug regimen; however in the overwhelming majority of cases small diameter synthetic grafts fail due to neointimal hyperplasia at the anastomoses. This ingrowth of tissue at an anastomosis is initiated by the migration and proliferation of smooth muscle cells (SMCs), partially due to the absence of a protective endothelial cell (EC) layer on the luminal surface of the graft. The presence of ECs would fundamentally alter the interaction between the graft surface and blood as well as reduce or prevent SMC migration and proliferation, ultimately improving long term graft patency. An additional benefit of confluent ECs on the graft lumen is that once exposed to physiological shear rates, a confluent EC surface is known to shift to a shear-induced anticoagulant and anti-platelet EC phenotype.[16] Indeed ECs have been seeded on fibrin glue-coated ePTFE grafts previously and shown to reduce neointimal hyperplasia formation.[17]

Poly(vinyl alcohol) (PVA) is one of many polymers which have been investigated as a potential synthetic graft biomaterial due to its biocompatibility, tunable mechanical properties, and inert surface properties.[18–21] PVA has recently been shown to be non-irritating to soft tissues, non-hemolytic, and non-cytotoxic.[22,23] However ECs do not readily adhere to PVA, ultimately restricting its biointegration. ECs and SMCs attach to- and proliferate on- ECM surfaces through cell adhesion molecules known as integrins. The chemical bonds which occur between the activated N-terminus of an integrin and the available reactive groups on a biomaterial surface ultimately govern EC adhesion, proliferation, differentiation, migration, and survival.[24] Amines and amides, as well as carbonyl groups on the biomaterial surface are required for peptide bonding between an integrin and the biomaterial surface. Critically, none of these reactive groups important for integrin binding are present on inert biomaterials including unmodified PVA.

Reactive ion plasma (RIP) is a process typically used to chemically or physically etch surfaces.[25] RIP-treatment has also been shown to significantly increase the hydrophilicity of other synthetic graft biomaterials through the introduction of polar groups.[25,26] Several groups have reported the effect of varying parameters such as power, treatment time, pressure, and gas mixture on the impregnation of amino groups on the surface of various polymers, but a comprehensive study of the effect of these parameters on surface modification of PVA biomaterials and platelet and endothelial cell attachment remains unexplored.[27–29] Previous studies on PVA have demonstrated that exposure to some nitrogen-containing plasmas increases EC attachment and density, but characterization of the effect of varying RIP parameters including carrier gas and power on the surface chemistry, cell adhesion, and thrombogenicity have yet to be reported.[21,25,30] Importantly, the thrombogenicity of the RIP-treated PVA biomaterials has not been reported previously in conjunction with cell studies. We present a more clinically-translatable and well-established model for testing thrombus generation on these surfaces using non-anticoagulated blood through an ex vivo shunt. In this study we tested the effect of carrier gas, as well as RIP power on the surface properties of PVA, primary EC attachment, and surface thrombogenicity in the stringent *ex vivo* model. We hypothesize that increasing the presence of nitrogen in the carrier gas and increasing RIP power would increase the surface nitrogen content of PVA, which in turn would enhance EC attachment and viability without affecting the thrombogenicity compared to untreated PVA.

2. Experimental Section

2.1 PVA Sample Preparation

Both flat and tubular samples were manufactured for these studies. Flat samples were used for surface characterization and cell attachment assays while tubular samples were used for *ex vivo* thrombosis testing in whole blood. Crosslinking of PVA was done as described previously.[20] In short, 10% (w/v) poly(vinyl alcohol) (85-124 kDa, 87-89% hydrolyzed) (SigmaAldrich, St. Louis, MO) was crosslinked with 15% (w/v) sodium trimetaphosphate (SigmaAldrich, St. Louis, MO) and 30% (w/v) NaOH. The crosslinking PVA solution was centrifuged to remove bubbles and immediately used for casting. PVA flat samples were cast in a 6 cm petri dish (Eppendorf, Hamburg, Germany) and were cured at 18°C - 20°C for 10 days. The cured flat samples were hydrated in PBS (Fisher Scientific, Waltham, MA) and DI Water then thoroughly rinsed in DI Water overnight. The flat samples were dried fully before further modification was performed. For fabrication of tubular PVA samples a cylindrical mold (OD=3.75 mm) was coated with a thin PDMS film (Dow Corning, Midland, MI). The PDMS film was then air plasma treated for 1 min and 20 sec at 85 W and 0.8 Nl/h. The mold was immediately immersed in crosslinking PVA solution. Repeated dip-casting was then performed in crosslinking PVA solution with a drying duration of 15-30 min between each dip. The tube was then cured at 18°C - 20°C for 3 days before hydration in PBS (Fisher Scientific, Waltham, MA) and DI Water, then thoroughly rinsed in DI Water overnight. The tube was then dehydrated before RIP treatment was performed.

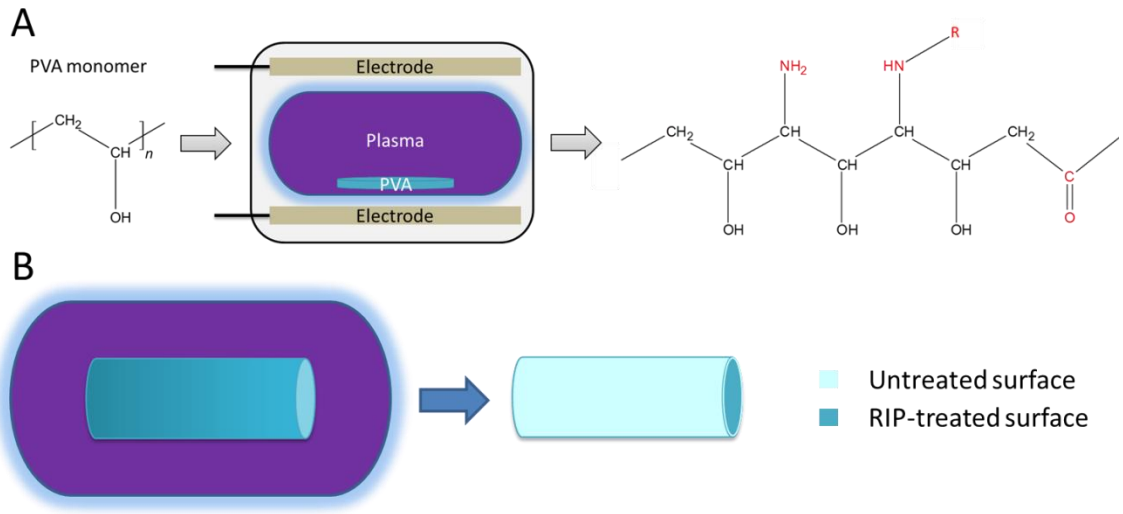

Figure 1: RIP treatment alters the surface chemistry of PVA. Amines and carbonyl groups, which provide binding sites for integrins, are formed on the surface (A). For *ex vivo* shunt studies PVA tubes were treated with RIP and inverted (B).

2.2 *Reactive Ion Plasma Treatment of PVA*

PVA samples were treated using a Plasma-Therm Batchtop VII (St. Petersburg, Florida, USA). A radiofrequency (RF) power of 50 W, 100 W, 150 W, or 300 W with a DC bias of 370 V and a pressure of 100 mTorr was used for all treatments. A total gas flow rate of 50 sccm was used for all studies. Oxygen, nitrogen, argon, and 5% H_2/N_2 were used for the RIP treatments. For the atmospheric mixture (Atm) 39 sscm of N_2 gas and 11 sccm of O_2 was used in order to maintain the total percent composition at 78% and 22%, respectively. Figure 1A depicts the treatment geometry for flat PVA samples. Untreated PVA was exposed to RIP treatment for 5 minutes. For the treatment of tubular samples, oxygen, nitrogen, or argon gases were used at an RF power of 100 W, DC bias of 370 V, and a flow rate of 50 sccm. The tubes were suspended in the plasma chamber and treated 5 minutes. Before use in the *ex vivo* shunt model, all tubular samples were inverted such that the treated surface constituted the luminal portion of the graft as depicted in Figure 1B.

2.3 *X-Ray Photoelectron Spectroscopy*

Surface nitrogen content was determined using x-ray photoelectron spectroscopy (XPS). XPS experiments were performed using a Versaprobe II (Physical Electronics, Chanhassen, Minnesota, USA) with an aluminum Kα monochromator source at 25.2 W. Survey spectra were acquired with 1.0 eV step and 117.4 eV pass energy, while high resolution elemental spectra (Figure 2) were acquired with 0.1 eV step and 23.5 eV pass energy. A scan area of 500 μm^2 was analyzed with pressure below 2 x 10^{-4} Pa. The detector was oriented at an angle of 45° to the sample surface. The amount of nitrogen, oxygen, and carbon present in the PVA surface were calculated as a percentage of the total. For example, the percent surface nitrogen was calculated as the ratio of the integral of the surface nitrogen peak to those of surface carbon, oxygen, and nitrogen for each sample, and a total of 5 samples were tested for each treatment. All XPS data was gathered within 14 days of RIP treatment.

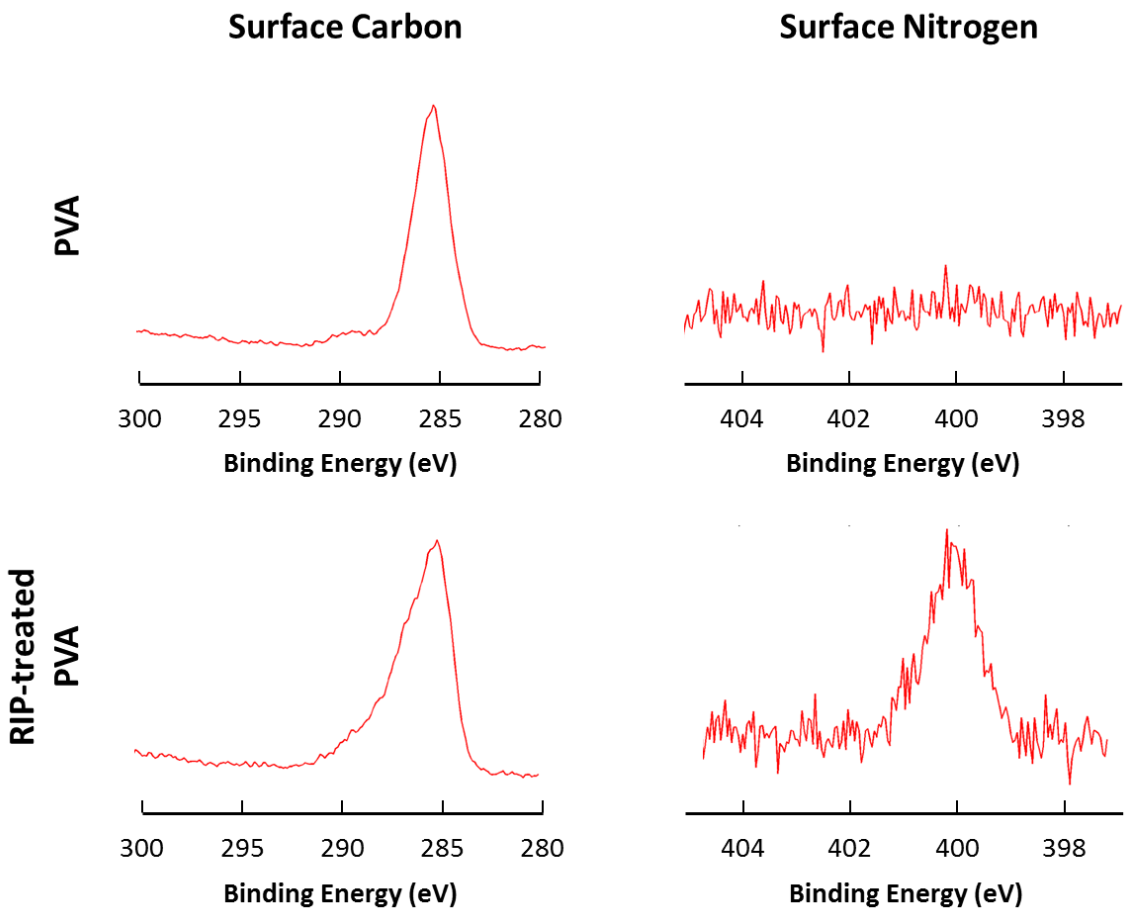

Figure 2: Representative high-resolution XPS spectra of surface nitrogen and carbon on native and RIP-treated PVA. Nitrogen appears on the surface of PVA after RIP treatment.

2.4 *Contact Angle Measurements*

Static contact angle measurements were all taken with PVA in the dried state using a custom imaging setup. The images were analyzed using ImageJ™. Three µL of DI water were deposited on the surface of a flat PVA sample and images were taken within 10 seconds to avoid absorption of water by the hydrogel. Measurements were taken at a non-specific location for each sample and four samples for each plasma treatment were measured.

2.5 *Endothelial Colony Forming Cell Culture*

Baboon endothelial colony forming cells (ECFCs) were isolated from peripheral blood as described previously by Hinds et al.[31] Briefly, the mononuclear cells were isolated from a venous blood draw using density gradient centrifugation (Histopaque 1077) and seeded on bovine fibronectin (Sigma-Aldrich, St. Louis, MO) in endothelial growth media (EGM)-2 (Lonza, Walkersville, MD) which was supplemented with 20% fetal bovine serum (FBS) (Hyclone, Logan, UT). The cultures were allowed to proliferate until outgrowth colonies were observed, which occurred between 7–21 days in culture. ECFCs were then passaged and expanded on bovine collagen I (MP Biomedicals, Santa Ana, CA) coated tissue culture flasks in EGM-2 supplemented with 10% FBS. CD31 positive ECFCs were bead sorted at passage 2 using Dynal magnetic beads (Invitrogen, Carlsbad, CA). Growth media was EGM-2 supplemented with 10% FBS in all studies. All cells were used between passage numbers 3–4 to seed 8 mm diameter PVA samples and cultured in a standard incubator at 37 °C and 5% CO_2. ECFCs were seeded at 100,000 cells per well in 48 well plate. Cells were grown for 48 hours, rinsed and immunostained.

2.6 *Immunostaining of ECFCs*

ECFCs were fixed in warm 3.7% paraformaldehyde in 48-well plates. Cells were permeabilized with 0.1% TritonX-100 for 10 min. Image-iT® FX Signal Enhancer (Invitrogen, Carlsbad, CA) was added to each well and incubated for 30 minutes followed by Alexa Fluor® 568 phalloidin (Invitrogen, Carlsbad, CA) diluted 1:200 in PBS for 1 hr. Wells were then blocked with 10% goat serum in Buffer #1 for 30min. VE-cadherin (Invitrogen, Carlsbad, CA) diluted 1:100 in PBS w/ Ca/Mg and 1% BSA was then added to each well and incubated for 1 hr, followed by anti-mouse IgG_1 Alexa Fluor® 488 diluted 1:500 in PBS w/ Ca/Mg. DAPI (Invitrogen, Carlsbad, CA) diluted 1:10,000 in PBS w/ Ca/Mg and 1% BSA was added to each well for 5 min. The PVA samples were then carefully mounted onto glass slides with ProLong® Gold Antifade (Invitrogen, Carlsbad, CA). The samples were allowed to cure at room temperature overnight prior to imaging.

2.7 *Picogreen Assay*

Picogreen assays were performed to quantify the number of cells which had attached and grown on the surface of 8mm diameter PVA after each RIP treatment. PVA samples were first RIP treated according to section 2.2 and 48-well plates (Corning, Corning, NY) were coated with Agarose to block any contact between ECFCs and the tissue-culture treated plastic surface after seeding. Well plates were then seeded according to section 2.5. Samples were then washed thoroughly with PBS in order to remove any unattached cells and frozen overnight at -20°C. Cells were then lysed with SDS, diluted in TE buffer, and dsDNA labeled using Quant-iT Picogreen reagent (ThermoFisher, Waltham, MA). dsDNA from ECFC-seeded PVA was quantified as fluorescence intensity from a standard curve of calf thymus DNA (Invitrogen, Carlsbad, CA).

2.8 *Thrombogenicity Characterization*

All animals were housed and cared for by Oregon National Primate Research Center (ONPRC) staff according to the *Guide to the Care and Use of Laboratory Animals* prepared by the Committee on Care & Use of Laboratory Animals of the Institute of Laboratory Animal Resources, National Research Council (International Standard Book, Number 0-309-05377-3, 1996) and as approved by the ONPRC Institutional Animal Care and Use Committee.

Shunt studies were performed on a femoral arteriovenous shunt as described previously.[32] Briefly, autologous platelets and homologous fibrinogen were radiolabeled with indium-111 and iodine-125, respectively, in a non-human primate (*papio anubis)*. Tubular untreated PVA, N_2 RIP-treated PVA, O_2 RIP-treated PVA, Ar RIP-treated PVA, ePTFE (clinical control), or collagen-coated ePTFE (positive control) were connected to the shunt loop. In the absence of anti-coagulant and anti-platelet therapy, blood flow was established at 100 ml/min using a clamp downstream of the graft. Platelet deposition was measured for 1 hr using a gamma camera with 1 min exposure time steps. Fibrinogen accumulation was quantified at the study endpoint after complete decay (>10 half-lives) of indium-111. A total of four

samples were tested for each RIP treatment and ePTFE, differences between groups were determined using a one-way repeated measures ANOVA with Tukey's *post hoc*.

2.9 *Statistical Analysis*

All quantitative measurements were performed using the number of replicate samples indicated in the figure caption. Statistical significance was evaluated using ANOVA with a Tukey's *post hoc* for multivariate samples unless otherwise stated. Contact angle data was evaluated using ANOVA with a Dunnett's *post hoc*. For platelet accumulation, statistical significance between groups was determined using a one-way repeated measures ANOVA with Tukey's post hoc. A *p* value of less than 0.05 was considered statistically significant for all statistical analysis. For all of the data presented in this manuscript, any two data points lacking statistically significant differences are assigned the same letter.

3. Results

3.1 *Nitrogen Content*

The surface nitrogen content was altered with O_2 plasma RF power at 50 W, 100 W, 150 W, and 300 W (Figure 3). Surface nitrogen increased from 50 W to 100 W, but remained constant for powers between 100 W and 300 W according to a one-way ANOVA with Tukey's post hoc ($p < 0.05$).

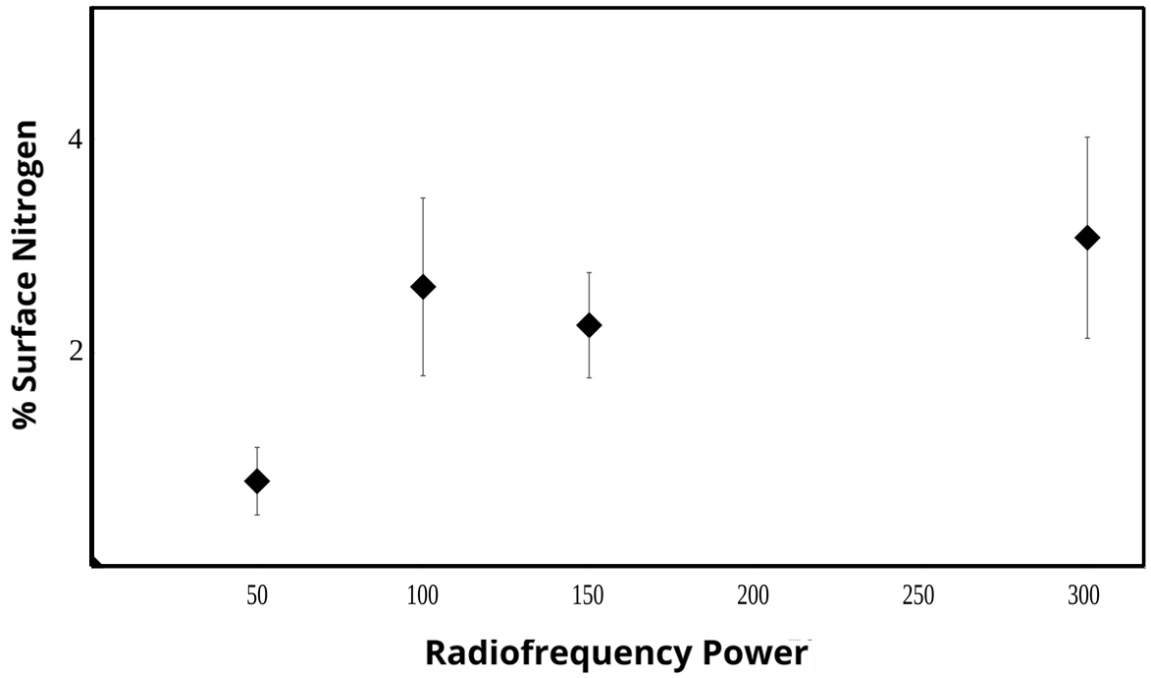

Figure 3: Surface nitrogen content on PVA treated with O_2 plasma as a function of RF power. Values approached steady state at values higher than 100 W according to a one-way ANOVA with equal variances ($N = 5$, $p < 0.05$).

Figure 4 shows the statistically significant increase of surface nitrogen content changes on PVA after each RIP treatment. The surface nitrogen content of untreated PVA was measured as a control and was 0.08% ± 0.08%. Treatment with 100 W N_2 yielded the highest surface nitrogen content (Figure 4, group E), followed by 50 W N_2, 100 W Atm, and 100 W 5% H_2/N_2 (Figure 4, group D). The surface nitrogen content was diminished for all other treatments according to their statistical groupings in Figure 4. Concomitant changes in surface oxygen and carbon for each RIP treatment are presented in Appendix A.

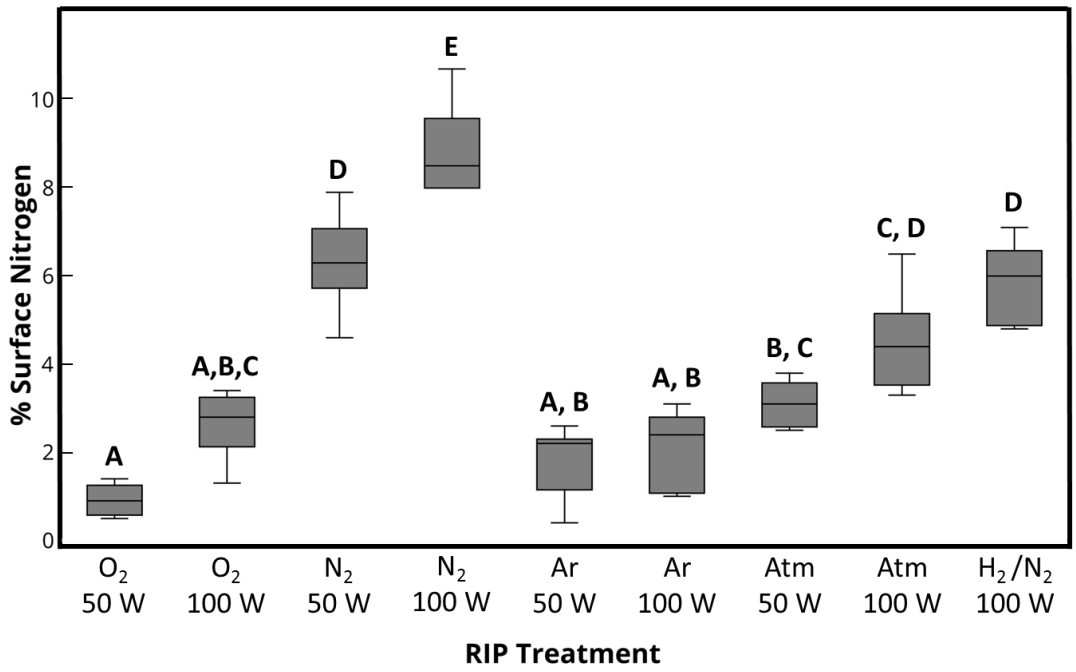

Figure 4: The surface nitrogen content of PVA is increased after 5 min RIP-treatment according to carrier gases and RF power. Groups which do not share a letter indicate that the null hypothesis (no statistical difference) can be rejected according to a one-way ANOVA with Tukey's post hoc ($N = 5$, $p < 0.05$).

3.2 *Contact Angle*

All RIP treatments significantly increased the wettability of PVA compared to untreated PVA (Table 1). N_2 RIP imparted the largest change, reducing the contact angle from 42.4° ± 1.1 to 17.8° ± 1.3 and 16.9° ± 2.5 for 50 W and 100 W, respectively. Oxygen, argon, and atmospheric mixture treatments also reduced the water contact angle of dried PVA according to Table 1.

Table 1: Contact angle measured on flat PVA samples for each RIP treatment. All treatments lowered the contact angle compared to untreated PVA to a statistically significant degree according to a one-way ANOVA with Dunnett's *post hoc* test (N = 4).

Plasma Treatment	50W	100W
Oxygen	30.4 ± 1.8	31.5 ± 3.1
Nitrogen	17.8 ± 1.3	16.9 ± 2.5
Argon	32.2 ± 2.0	28.6 ± 1.1
Atmospheric mixture	26.8 ± 1.7	25.5 ± 3.3
Untreated		42.4 ± 1.1

3.3 *Cell Affinity*

Untreated PVA did not support cell attachment and growth (Figure 5). RIP treatments of 100 W O_2 and 50 W N_2 were not shown to significantly increase ECFC attachment compared to untreated PVA (Figure 5, group D). Both Ar plasma treatments at 50 W and 100 W , as well as 100 W N_2 and 50 W O_2 plasmas, increased ECFC attachment significantly, compared to untreated PVA (Figure 5, group A). Thus, all RIP treatments increased or maintained ECFC attachment compared to untreated PVA.

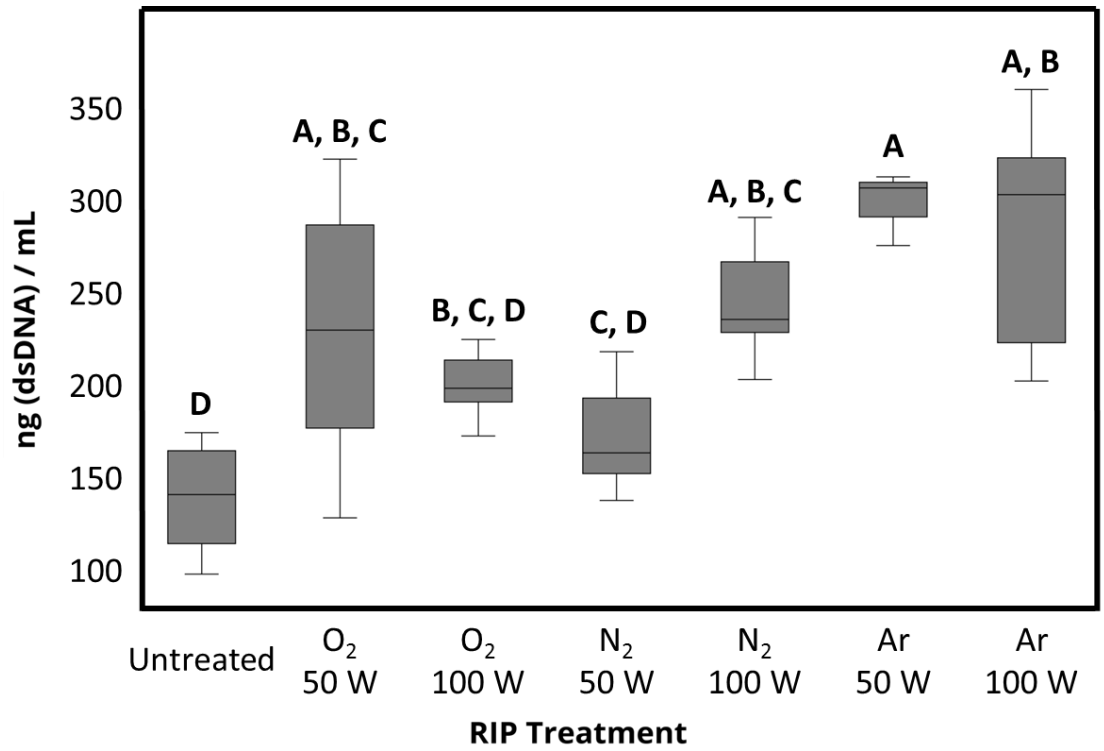

Figure 5: Attachment of primary ECFCs on RIP-treated PVA. All RIP treatments support EC attachment compared to untreated PVA and Argon RIP treatments increase cell attachment most significantly of the carrier gases tested. Groups which do not share a letter indicate that the null hypothesis (no statistical difference) can be rejected according to a one-way ANOVA with Tukey's post hoc ($N = 5$, $p < 0.05$).

Figure 6 shows representative three-channel fluorescent images (A-C) and one composite image (D) of ECFC attachment to 100 W N_2 RIP-treated PVA. Blue fluorescence indicates cell nuclei, red: actin filaments, and green: VE-cadherin. Figure 6A indicates localized confluence at 20X magnification for the RIP treatment and Figure 6B shows the presence of VE-cadherin indicating tight cell junctions in the ECFC culture.

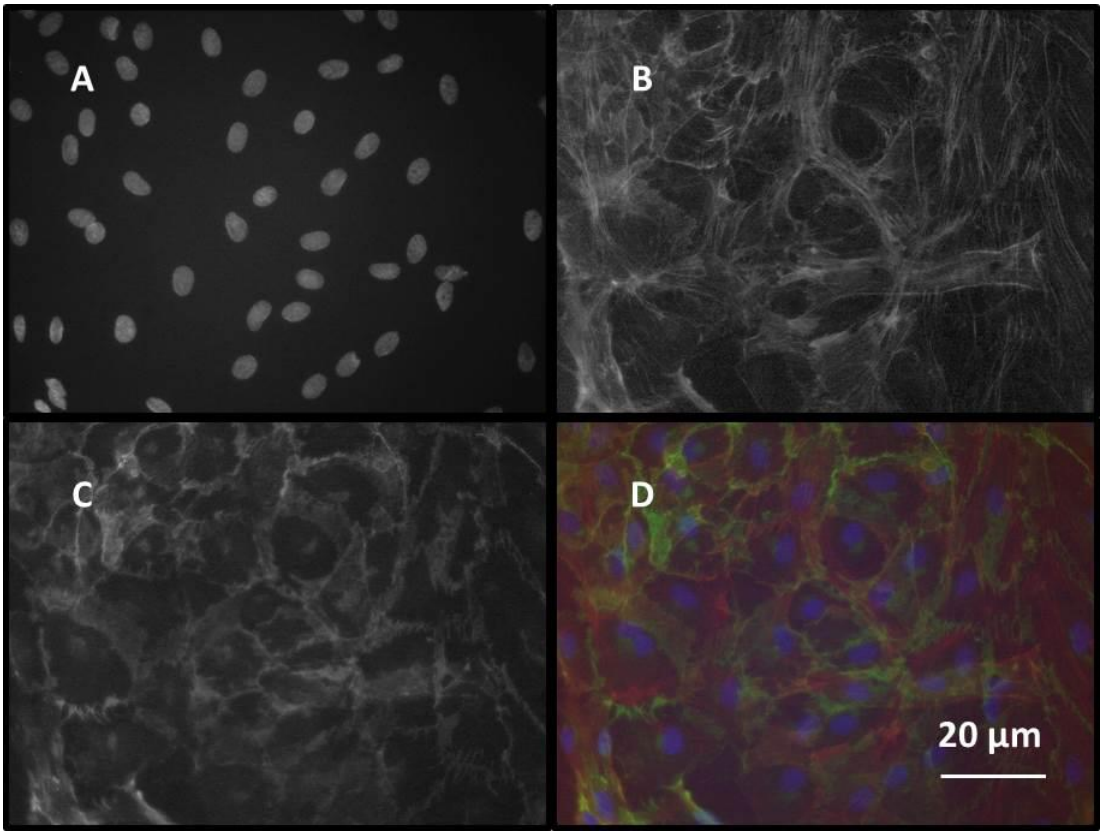

Figure 6: Representative fluorescence images of ECFCs cultured on 100 W N_2 RIP-treated PVA at 20X magnification. In composite image (D) the images are colored, with blue indicating cell nuclei (A), red: actin filaments (B), and green: VE-cadherin (C).

3.4 *Thrombogenicity Characterization*

Figure 7 shows platelet and fibrin (inset) accumulation over 1 hr of testing with whole, non-anticoagulated blood, flowing at 100mL/min. Tubular PVA samples with and without RIP treatment were compared to clinical grade ePTFE and collagen-coated ePTFE as negative and positive controls, respectively. A single collagen-coated sample was tested (black crosses) and agreed with historic data[20,32] confirming consistency within the testing system. RIP treatment with 100 W N_2 was shown to significantly decrease both platelet and fibrin accumulation compared to ePTFE. Untreated PVA was shown to decrease platelet accumulation but not fibrin content compared to ePTFE, 100 W Ar RIP was not shown to decrease platelet accumulation, but did significantly decrease the fibrin content of the thrombus compared to ePTFE. The 100 W O_2 plasma PVA were not significantly different in either platelet or fibrin accumulation

compared to ePTFE. Compared to untreated PVA, all RIP treatments did not significantly change platelet or fibrin accumulation.

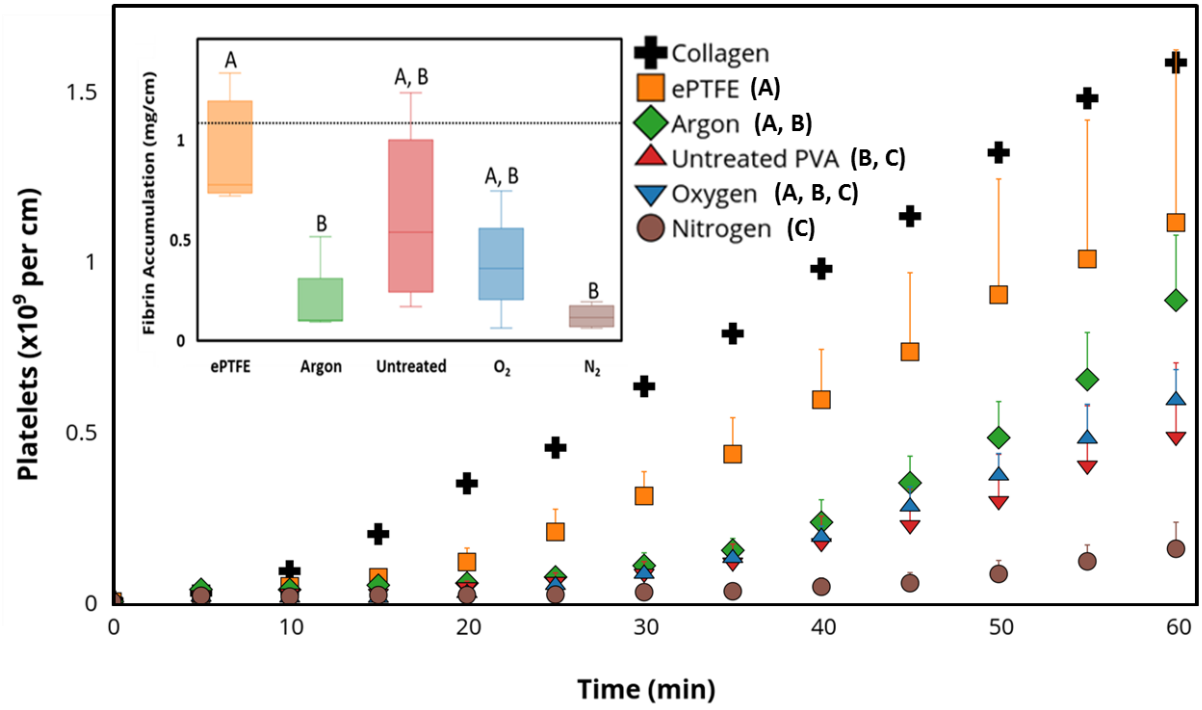

Figure 7 Platelet deposition and fibrin accumulation (Inset) over 1 hr of whole blood exposure in a non-human primate model of thrombosis. The mean difference of platelet accumulation was significantly lower for untreated PVA and nitrogen RIP treated samples relative to ePTFE. For platelet accumulation, statistical significance between groups was determined using a one-way repeated measures ANOVA with Tukey's post hoc (N = 4, $p < 0.05$). Fibrin accumulation for all graft materials and treatments were less than the positive collagen control (black dotted line, inset), according to a one-way ANOVA with Tukey's post hoc (N = 4, $p < 0.05$). For both analyses, groups which do not share a letter indicate that the null hypothesis (no statistical difference) can be rejected.

4. Discussion

The type of gas and power of RIP treatment were systematically tested to determine the changes in hydrogel properties, the ability to support EC attachment and growth, and the degree to which coagulation was initiated on the surface. Using O_2 plasma RIP treatments, the effect of the power of RIP treatment on the surface nitrogen content plateaued above 100 W. Non-nitrogen containing RIP treatments generally resulted in less surface nitrogen. The samples treated with 50 W and 100 W N_2, as well as the 100 W Atm

and H_2/N_2 samples had the highest average percentages of surface nitrogen content. Nitrogen-containing RIP treatment significantly decreased the water contact angle compared to untreated PVA; the N_2 treatment also decreased the water contact angle to a greater extent than the plasma treatments without N_2 confirming that increased surface nitrogen, in the form of polar amino groups, increases hydrogel wettability.

RIP has been shown to alter the surface of polymeric materials both chemically and physically.[25,33] These changes are imparted when charged particles, radicals, and electrons from the RIP interact with the polymeric substrate and ablate or replace surface polymer groups. The electronegativity of the carrier gas and the RF power significantly affect the number of free electrons in the RIP and therefore the degree of surface modification.[33] It has been noted anecdotally that the chemical and physical changes imparted on a polymeric surface depend on RIP power and carrier gas. However the details of this process and how they determine EC attachment and thrombogenesis have been poorly understood in part because most RIP modifications increase the wettability of a surface and therefore cell adhesion. However the relative importance of each RIP parameter as it relates to EC attachment and thrombogenesis has not been previously explored systematically.

PVA alone has been shown to not support EC attachment, previously.[25] Here, 50 W O_2, 100 W N_2, as well as 50 W and 100 W Ar RIP-treatments did support primary ECFC attachment on PVA significantly compared to untreated PVA. However the increase in surface nitrogen did not directly correlate with increased attachment of ECFCs as was hypothesized. This result indicates that the absolute number of amines available for integrin binding does not govern ECFC attachment alone. Interestingly, the introduction of surface nitrogen by 50 W N_2 RIP treatment for 1 minute was shown previously to increase human umbilical vein EC line EA.hy926 attachment to micropatterned PVA, yet the cells did not form a monolayer until 6 days in culture.[21] Importantly, in that study, micropatterned surfaces were required for cell-junctions to form. The micro and nano features, which approximate the hierarchical physical structure of ECM, have been shown to support EC growth to various degrees.[34] Physical etches such as Ar RIP have also been shown to alter the nanotopography of PVA,[25] and our data using primary ECFCs is consistent with previous studies showing increased EC adhesion to nanopatterned surfaces,[35] which were independent of RIP power. Although the degree of physical modification of the PVA surface with various RIP treatments was not quantified here, the physical surface modification caused by Ar RIP is likely to be

responsible for this increased EC affinity. A possible mechanism is that hierarchical surface texture introduced by RIP treatment increases cell migration and proliferation by promoting integrin attachment through cellular sub structures such as filopodia and lamellipodia more readily than amines alone. The interplay between the physical modification of the PVA surface along with the introduction of amines and carbonyl groups after RIP treatment is likely responsible for the difference in ECFC attachment among RIP treatments.

EC attachment and proliferation are known to be driven by integrins, transmembrane heterodimers with an α and β subunit, which bind to a surface through the formation of peptide bonds. Integrins are also known to vary considerably among cell types and phenotypes in their individual structures, chemistries, and ligand compliments, and therefore binding and signaling motifs. It is the peptide bonding between integrins and the RIP-altered surface properties that is implicated here in increased EC attachment after RIP treatment. This mechanism could be acting to bind directly with the activated N-terminus of integrins on the ECFCs, or it could be acting by increasing adsorption of extracellular matrix to the PVA surface which in turn increases integrin binding. ECs, SMCs, and platelets each have unique sets of integrins to bind to surfaces according to their cell type and phenotype and this work provides important characterization of RIP-treated PVA which can be used to tune the surface of PVA to preferentially promote primary EC affinity, prevent platelet attachment, and restrict SMC proliferation and migration. This knowledge is key to reducing the two major failure modes in small diameter graft synthetic grafts: neointimal hyperplasia and thrombosis.

Any cardiovascular biomaterial must be non-thrombogenic in order to avoid activation of coagulation factors and rapid occlusion due to the recruitment of platelets and fibrinogen, a process which can cause the loss of graft patency in a matter of hours. Many modifications of polymeric biomaterials which allow for the attachment of ECs, such as collagen coating, also dramatically increase platelet attachment due to the similarities in binding of their adhesion molecules to the sites on the surface modification. The binding of platelets can be measured using several assays with varying degrees of correlation to coagulation *in vivo*. Those assays include static assays, *in vitro* flow assays, and the shunt model presented in this paper. The *ex vivo* shunt model provides the most conclusive evidence to date that RIP treatments do not increase thrombogenicity of PVA and that the overall thrombogenicity of N_2 RIP-

treated PVA is significantly diminished compared to the clinical standard ePTFE. The data also suggest that RIP-treatment plays an important role in determining not only the size of a thrombus but also its composition. Specifically, on 100 W Ar treated PVA, while the number of platelets were not significantly decreased in the thrombi compared to ePTFE, the amount of fibrin did significantly decrease. Thus the overall thrombus burden or thombogenicity of the surface is dependent on the chemical and topographical changes imparted on PVA by RIP treatment.

5. Conclusions

This paper considers for the first time the effect of systematic chemical and physical RIP etches by varying the power and carrier gas on primary EC attachment and thrombogenicity on flat and tubular PVA. Treating PVA with RIP is shown to alter its surface chemistry according to the power and carrier gas. N_2 RIP treatments were particularly effective at increasing surface nitrogen content and altering the hydrophilicity of the surfaces while Ar RIP treatments also notably increased the wettability of PVA. These changes to the PVA surface increased its affinity to ECFCs and did not compromise thrombogenicity in a clinically relevant model. The mechanism of increased EC affinity acts partially through physical affinity for cellular sub-structures and partially through chemical affinity for specific integrins. Furthermore, the parameters of RIP have the potential to be tuned to impart specific integrin affinities and promote EC attachment while restricting SMC attachment, ultimately providing a simple manufacturing process to reduce neointimal hyperplasia.

Acknowledgments

This work is supported by the Nation Institutes of Health R01HL130274, R01DE026170, and R01HL144113. The authors declare that they have no competing interests.

Appendix A. Supplementary data

Supplemental Table 1: Surface nitrogen, oxygen, and carbon of PVA after RIP treatment. Each value is the mean ± the standard deviation (N = 5).

Surface Nitrogen					
Plasma Treatment	50W	50W (45 days)	100W	100W (45 days)	
Oxygen	0.9 ± 0.4	0.8 ± 1.5	2.6 ± 0.8	3.8 ± 3.4	
Nitrogen	6.3 ± 1.2	5.5 ± 1.9	8.9 ± 1.1	5.4 ± 1.8	
Argon	1.8 ± 0.9	1.4 ± 1.4	2.1 ± 1.0	1.0 ± 1.2	
Atmospheric mixture	3.3 ± 0.5	3.5 ± 1.6	4.5 ± 1.3	0.8 ± 0.7	
H_2/N_2			5.8 ± 1.0	1.4 ± 1.2	
Untreated					0.08 ± 0.08
Surface Oxygen					
Plasma Treatment	50W	50W (45 days)	100W	100W (45 days)	
Oxygen	32.8 ± 3.9	22.6 ± 10	33.4 ± 5.8	32.4 ± 6.0	
Nitrogen	21.3 ± 6.0	25.8 ± 6.0	26.8 ± 2.0	33.6 ± 5.9	
Argon	27.4 ± 7.7	25.8 ± 5.0	28.7 ± 5.1	27.2 ± 6.0	
Atmospheric mixture	34.8 ± 3.3	32.5 ± 1.3	34.3 ± 4.0	24.8 ± 7.8	
H_2/N_2			30.0 ± 9.4	17.0 ± 4.9	
Untreated					28.8 ± 3.9
Surface Carbon					
Plasma Treatment	50W	50W (45 days)	100W	100W (45 days)	
Oxygen	66.6 ± 4.0	76.6 ± 9.9	64.0 ± 5.8	63.7 ± 5.3	
Nitrogen	72.4 ± 6.8	68.6 ± 7.3	64.2 ± 1.9	61.0 ± 7.5	
Argon	70.8 ± 8.4	72.9 ± 5.3	69.3 ± 5.7	71.8 ± 6.7	
Atmospheric mixture	61.9 ± 3.5	63.9 ± 2.1	61.6 ± 4.1	74.3 ± 8.4	
H_2/N_2			64.2 ± 9.4	81.7 ± 6.0	
Untreated					71.1 ± 4.0

References

1. Zoghbi, W. A., Duncan, T., Antman, E., Barbosa, M., Champagne, B., Chen, D., Gamra, H., Harold, J. G., Josephson, S., Komajda, M., … Wood, D. A. Sustainable Development Goals and the future of cardiovascular health. A statement from the Global Cardiovascular Disease Taskforce. *Eur. Heart J.* **35,** 3238–9 (2014).

2. Mozaffarian, D., Benjamin, E. J., Go, A. S., Arnett, D. K., Blaha, M. J., Cushman, M., Das, S. R., de Ferranti, S., Després, J.-P., Fullerton, H. J., … Turner, M. B. Heart Disease and Stroke Statistics—2016 Update. *Circulation* (2015).

3. Klinkert, P., Post, P. ., Breslau, P. . & van Bockel, J. . Saphenous Vein Versus PTFE for Above-Knee Femoropopliteal Bypass. A Review of the Literature. *Eur. J. Vasc. Endovasc. Surg.* **27,** 357–362 (2004).

4. Harskamp, R. E., Lopes, R. D., Baisden, C. E., de Winter, R. J. & Alexander, J. H. Saphenous Vein Graft Failure After Coronary Artery Bypass Surgery. *Ann. Surg.* **257,** 824–833 (2013).

5. Sarkar, S., Salacinski, H. J., Hamilton, G. & Seifalian, A. M. The Mechanical Properties of Infrainguinal Vascular Bypass Grafts: Their Role in Influencing Patency. *Eur. J. Vasc. Endovasc. Surg.* **31,** 627–636 (2006).

6. Fitzpatrick, L. E. & McDevitt, T. C. Cell-derived matrices for tissue engineering and regenerative medicine applications. *Biomater. Sci.* **3,** 12–24 (2015).

7. Pashneh-Tala, S., MacNeil, S. & Claeyssens, F. The Tissue-Engineered Vascular Graft-Past, Present, and Future. *Tissue Eng. Part B. Rev.* **22,** 68 (2015).

8. Moroni, F. & Mirabella, T. Decellularized matrices for cardiovascular tissue engineering. *Am. J. Stem Cells* **3,** 1–20 (2014).

9. Gui, L., Muto, A., Chan, S. A., Breuer, C. K. & Niklason, L. E. Development of Decellularized Human Umbilical Arteries as Small-Diameter Vascular Grafts. *Tissue Eng. Part A* **15,** 2665–2676 (2009).

10. Robinson, K. A., Li, J., Mathison, M., Redkar, A., Cui, J., Chronos, N. A. F., Matheny, R. G. & Badylak, S. F. Extracellular matrix scaffold for cardiac repair. *Circulation* **112,** I135-43 (2005).

11. Brewster, D. C. Current controversies in the management of aortoiliac occlusive disease. *J. Vasc. Surg.* **25,** 365–79 (1997).

12. Chlupác, J., Filová, E. & Bacáková, L. Blood vessel replacement: 50 years of

development and tissue engineering paradigms in vascular surgery. *Physiol. Res.* **58 Suppl 2,** S119-39 (2009).

13. Desai, M., Seifalian, A. M. & Hamilton, G. Role of prosthetic conduits in coronary artery bypass grafting. *Eur. J. Cardio-Thoracic Surg.* **40,** 394–398 (2011).

14. Sarkar, S., Sales, K. M., Hamilton, G. & Seifalian, A. M. Addressing thrombogenicity in vascular graft construction. *J. Biomed. Mater. Res. Part B Appl. Biomater.* **82B,** 100–108 (2007).

15. Ariyoshi, H., Okuyama, M., Okahara, K., Kawasaki, T., Kambayashi, J., Sakon, M. & Monden, M. Expanded polytetrafluoroethylene (ePTFE) vascular graft loses its thrombogenicity six months after implantation. *Thromb. Res.* **88,** 427–33 (1997).

16. Ensley, A. E., Nerem, R. M., Anderson, D. E. J., Hanson, S. R. & Hinds, M. T. Fluid shear stress alters the hemostatic properties of endothelial outgrowth cells. *Tissue Eng. Part A* **18,** 127–36 (2012).

17. Deutsch, M., Meinhart, J., Zilla, P., Howanietz, N., Gorlitzer, M., Froeschl, A., Stuempflen, A., Bezuidenhout, D. & Grabenwoeger, M. Long-term experience in autologous in vitro endothelialization of infrainguinal ePTFE grafts. *J. Vasc. Surg.* **49,** 352–362 (2009).

18. Millon, L. E., Nieh, M.-P., Hutter, J. L. & Wan, W. SANS Characterization of an Anisotropic Poly(vinyl alcohol) Hydrogel with Vascular Applications. doi:10.1021/ma062781f

19. Tallawi, M., Boccaccini, A. R., Rosellini, E., Barbani, N., Cascone, M. G., Rai, R. & Saint-Pierre, G. Strategies for the chemical and biological functionalization of scaffolds for cardiac tissue engineering: a review. doi:10.1098/rsif.2015.0254

20. Cutiongco, M. F. A., Anderson, D. E. J., Hinds, M. T. & Yim, E. K. F. In vitro and ex vivo hemocompatibility of off-the-shelf modified poly(vinyl alcohol) vascular grafts. *Acta Biomater.* **25,** 97–108 (2015).

21. Cutiongco, M. F. A., Goh, S. H., Aid-Launais, R., Le Visage, C., Low, H. Y. & Yim, E. K. F. Planar and tubular patterning of micro and nano-topographies on poly(vinyl alcohol) hydrogel for improved endothelial cell responses. *Biomaterials* **84,** 184–195 (2016).

22. Alexandre, N., Ribeiro, J., Gärtner, A., Pereira, T., Amorim, I., Fragoso, J., Lopes, A., Fernandes, J., Costa, E., Santos-Silva, A., … Luís, A. L. Biocompatibility and hemocompatibility of polyvinyl alcohol hydrogel used for vascular grafting- *In vitro* and *in vivo* studies. *J. Biomed. Mater. Res. Part A* **102,** n/a-n/a (2014).

23. Lamponi, S., Leone, G., Consumi, M., Greco, G. & Magnani, A. In Vitro Biocompatibility

of New PVA-Based Hydrogels as Vitreous Body Substitutes. *J. Biomater. Sci. Polym. Ed.* **23,** 555–575 (2012).

24. Moreno-Layseca, P. & Streuli, C. H. Signalling pathways linking integrins with cell cycle progression. *Matrix Biol.* **34,** 144–153 (2014).

25. Ino, J. M., Chevallier, P., Letourneur, D., Mantovani, D. & Le Visage, C. Plasma functionalization of poly(vinyl alcohol) hydrogel for cell adhesion enhancement. *Biomatter* **3,**

26. Valence, S. de, Tille, J.-C., Chaabane, C., Gurny, R., Bochaton-Piallat, M.-L., Walpoth, B. H. & Möller, M. Plasma treatment for improving cell biocompatibility of a biodegradable polymer scaffold for vascular graft applications. *Eur. J. Pharm. Biopharm.* **85,** 78–86 (2013).

27. Calderon, J. G., Harsch, A., Gross, G. W. & Timmons, R. B. Stability of plasma-polymerized allylamine films with sterilization by autoclaving. *J. Biomed. Mater. Res.* **42,** 597–603 (1998).

28. Gancarz, I., Bryjak, J., Poźniak, G. & Tylus, W. Plasma modified polymers as a support for enzyme immobilization II. Amines plasma. *Eur. Polym. J.* **39,** 2217–2224 (2003).

29. Gomathi, N., Sureshkumar, A. & Neogi, S. RF plasma-treated polymers for biomedical applications. *Current Science* **94,** 1478–1486

30. Latkany, R., Tsuk, A., Sheu, M. S., Loh, I. H. & Trinkaus-Randall, V. Plasma surface modification of artificial corneas for optimal epithelialization. *J. Biomed. Mater. Res.* **36,** 29–37 (1997).

31. Hinds, M. T., Ma, M., Tran, N., Ensley, A. E., Kladakis, S. M., Vartanian, K. B., Markway, B. D., Nerem, R. M. & Hanson, S. R. Potential of baboon endothelial progenitor cells for tissue engineered vascular grafts. *J. Biomed. Mater. Res. Part A* **86A,** 804–812 (2008).

32. Anderson, D. E. J., Glynn, J. J., Song, H. K. & Hinds, M. T. Engineering an Endothelialized Vascular Graft: A Rational Approach to Study Design in a Non-Human Primate Model. *PLoS One* **9,** e115163 (2014).

33. Phan, L., Yoon, S. & Moon, M.-W. Plasma-Based Nanostructuring of Polymers: A Review. *Polymers (Basel).* **9,** 417 (2017).

34. Lin, X., Shi, Y., Cao, Y., Wieringa, P., Tonazzini, I., Micera, S., Wu, K.-C., Tseng, C.-L., Wu, C.-C., Fozdar, D. Y., … Guck, J. From nano to micro: topographical scale and its impact on cell adhesion, morphology and contact guidance. *J. Phys. Condens. Matter* **28,**

35. Hwang, S. Y., Kwon, K. W., Jang, K.-J., Park, M. C., Lee, J. S. & Suh, K. Y. Adhesion

Assays of Endothelial Cells on Nanopatterned Surfaces within a Microfluidic Channel. *Anal. Chem.* **82,** 3016–3022 (2010).